Engineering Geology 224 (2017) 97–104

Contents lists available at ScienceDirect

Engineering Geology

journal homepage: www.elsevier.com/locate/enggeo

Application of laser scanning for rapid geologic documentation of trench exposures

J.Y. Han, N.J. Huang, J.T.Y. Chuang*

Department of Civil Engineering, National Taiwan University, Taiwan

A R T I C L E I N F O

Keywords:
Terrestrial LiDAR
Trench excavation
Image analysis
Image classification
Grain-size analysis

A B S T R A C T

Trenching of a known or inferred fault is a traditional technique to verify the presence of the fault and potentially determine relative palaeoseismic slip rates and magnitudes. These procedures have been employed and improved over the past 50 years and have been particularly applied by engineering geologists concerned with local and regional tectonics that affect large structures such as dams and power plants as well as local habitable structures. Traditionally, however, trench excavation and documentation (logging) is time-consuming and laborious, requiring experienced geologists to identify plausible trench locations and to manually document the exposures in the field. Differences of interpretation are common; hence, many jurisdictions require an independent reviewer to field check trench exposures and to assess the reasonableness of the geologic interpretations. In this paper, we describe a less costly, novel technique to enhance the quality and rapidity of geologic trench documentation. Specifically, we use terrestrial Light Detection and Ranging (LiDAR) scans, coupled with camera imagery, to collect three-dimensional point clouds. These data are then converted into trench-wall images that are readily accessible for analysis even after trench closure. The procedure also provides grain-size (texture) data that are useful for identification and correlation of discrete, trench-exposed stratigraphic markers that are offset or that overlie an imaged fault without being broken. Then, depending on sediment dating, a fault can be deemed “active” or “hazardous” depending on the local classification, and this information can thus be used by planners and others involved in hazard and risk reduction.

1. Introduction

An active fault is likely to experience another earthquake sometime in the future (Slemmons and Defolo, 1986). Therefore, understanding the distribution of faults is of particular importance for the study of earthquakes and hazard assessment. Starting from the late 1950s, thousands of trenches, ranging from small 2-m-deep backhoe trenches to 12-m-deep excavator exposures, have been emplaced in urban areas as required by local regulations for building permits.

Even though the level of seismic hazard analysis has improved in the last few decades, the mechanisms controlling the occurrence of earthquakes remain unclear. Analysis of observations of geodetic, tidal, and crustal changes acquired before and after earthquakes is the conventional method of investigating the occurrence of earthquakes. In recent decades, palaeoseismology studies have concentrated on analysing the long-term slip rate and estimating the probability as well as the severity of future earthquakes (Matsuda, 1977; Talwani and Cox, 1985; McCalpin, 1996, 2009). These studies not only compensate for the lack of instruments and historical earthquake records but also provide useful information for regional to local seismic hazard analysis. Unfortunately, little success has been attained thus far other than generalisations of prediction. Indeed, no method can accurately predict the time, place, and magnitude of an earthquake, but considerable progress has been made in the study of ancient earthquakes and the recurrence period of earthquakes (Sieh, 1978; Ran et al., 2010; Chen et al., 2001).

The current mainstream method of earthquake prediction is to understand the historical evidence for earthquake events in order to estimate the possible recurrence period in the future. Investigations involve excavating fault trenches at suitable sites, considering legal access, surface geomorphic expression, the presence and thickness of local sediment accumulation, and the potential for exposing relatively datable stratigraphic markers. The excavation procedures commonly comprise the following steps: (i) identification of an active fault; (ii) selection of a trenching site; (iii) contact with local authorities; (iv) construction of a fence surrounding the trench site; (v) preparation of trench walls for mapping; (vi) gridding of trench walls; (vii) marking locations of mapped features with coloured nails; (viii) mapping trench

* Corresponding author.
E-mail address: jtychuang@ntu.edu.tw (J.T.Y. Chuang).

http://dx.doi.org/10.1016/j.enggeo.2017.05.010
Received 6 February 2017; Received in revised form 16 May 2017; Accepted 16 May 2017
Available online 17 May 2017

walls (photo stitching/mosaic); (ix) sampling and packaging of datable material; (x) backfilling of trench; (xi) C14-dating of collected samples.

However, fault excavation has high cost and often faces weather and working-space constraints as well as problems relating to land ownership. Moreover, the field conditions of a trench are rarely preserved as detailed three-dimensional (3D) geospatial data for long-term investigation. Once the earthwork is backfilled, the information about the trench will only remain in the relevant two-dimensional (2D) documents. This implies that it would be hard to achieve an integrated analysis for further geological investigation if more evidence were discovered.

Regarding the issues mentioned above, our study constructed a scheme that uses terrestrial Light Detection and Ranging (LiDAR) techniques for contactless measurement to preserve the 3D geological data coupled with RGB spectral information of the trench. Compared to the traditional grid process (cf. Pantosti and Yeats, 1993), our approach improves the working efficiency and the accuracy in producing images of trench walls without destroying the trench surfaces. Trench wall images are obtained by projecting the 3D points onto their best-fit projection plane. Further, a grain-size (texture) classification is performed to identify different categories of lithological features in the trench wall image, which will help geologists to determine the locations of fault lines. Traditionally, 3D trench imaging emplaces and logs parallel trenches to identify offset channels, beds, and other so-called piercing points that can be relatively dated and hence used for assessing long-term slip rates. In contrast, once a fault line has been determined from two or more trench wall images during the proposed procedure, a 3D trench plane can be established efficiently by fitting all 3D points belonging to each fault line. Unlike the traditional logs in which a strike of a fault is merely determined from one viewpoint, 3D trench imaging can provide both elevation angle and azimuth; this, in turn, can lead to a more comprehensive interpretation and visualisation of the trace evidence of fault movement.

The aim of this work is to describe a new approach that facilitates trench analysis by reducing human-made damage to the trench during the construction process and lessens the misjudgements in identifying and interpreting the stratification. The advantages of the new approach are illustrated by a case study example of an important active fault in Taiwan.

2. Methodology

As shown in Fig. 1, the workflow of the proposed procedure comprised five steps, namely data pre-processing, best-fit plane projection, trench image production, grain-size (texture) classification, and 3D trench plane generation. The data pre-processing involved the procedures of point cloud registration and noise removal. Registration was performed to register multiple LiDAR scans onto the same coordinate system so as to reduce the obstructed areas and obtain a

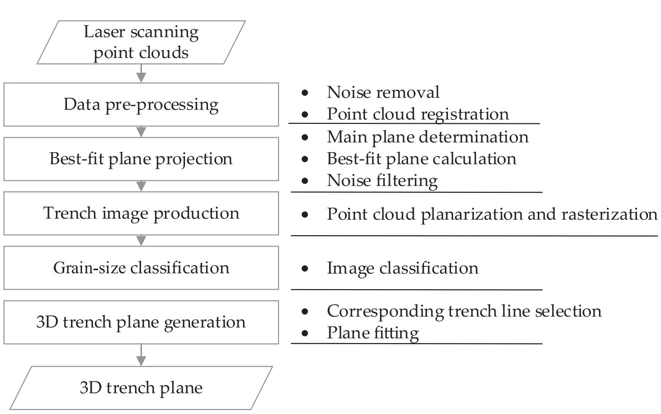

Fig. 1. The workflow of the proposed procedure.

complete view of the targeted region. The points in the non-target area should be treated as noise and removed. The registration process encourages data consistency and data completion. Typically, the manufacturer of the LiDAR system provides tools for data editing and registration. Also, lots of open-source software applications using algorithms such as ICP (Besl and McKay, 1992) or NISLT (Han, 2010) can be found. In this study, Trimble RealWorks (Trimble, 2013) was adopted for managing the point clouds to refine the targeted data used for the search for the best-fit projection plane.

2.1. The best-fit plane projection

Most fault-finding trenches are excavated with vertical walls, usually no more than 1.524 m high, conforming to safety standards. If they are deeper than this, hydraulic shoring is usually used to reduce the potential for wall collapse. On the other hand, some trench walls are constructed with an inclined angle and divided into several layers to avoid the natural collapse of the walls. Nevertheless, in practice, trench walls constructed by either method require that the best-fit projection plane be found for well projection geometry. As shown in Fig. 2, we characterised near vertical and oblique walls as inclined planes, and the trench floors were described as pathway planes in this study. The best-fit projection plane for the inclined plane was defined as a plane that formed the orthographic projection of the inclined plane. Under the assumption that the number of scanning points belonging to the inclined planes was larger than the number of scanning points belonging to pathway planes, the normal vector of the best-fit projection plane was explored by the vector geometry of the inclined and pathway planes. The point cloud can be rarefied according to the amount of data as long as the relative proportion remains, easing the computational burden. A 3D Delaunay triangulation was implemented on the points, and the normal vectors of each triangle were computed. Afterwards, a repeated process started with clustering on the normal vectors of each triangle.

The mean normal vector of the second largest group was deemed as the normal vector of the pathway plane regarding the previous assumption. A repeated check on the angles included between all the normal vectors in the selected group and the mean normal vector was conducted. Only the normal vector, whose included angle was smaller than a pre-defined tolerance, was retained and used to compute the new mean normal vector for the next iteration. The tolerance should be given based on the slant angles of the trench planes during the excavation and smaller than the difference between slope angles of each trench layer. The repeated process terminated when there was no vector eliminated from the accepted vector group. The final mean vector was deemed as the normal vector of the pathway planes $\overrightarrow{nv_p}$.

On the other hand, the same process can be utilised to find the normal vector of the inclined planes $\overrightarrow{nv_i}$. $\overrightarrow{nv_p}$ and $\overrightarrow{nv_i}$ were then used to derive the normal vector of a vertical plane $\overrightarrow{nv_v}$ by applying the cross product, $\overrightarrow{nv_v} = \overrightarrow{nv_p} \times \overrightarrow{nv_i}$. Similarly, the normal vector of the best-fit projection plane $\overrightarrow{nv_b}$ can be derived using the cross product of $\overrightarrow{nv_v}$ and $\overrightarrow{nv_p}$: $\overrightarrow{nv_b} = \overrightarrow{nv_v} \times \overrightarrow{nv_p}$.

2.2. Trench image production

Once the best-fit projection plane has been determined, the 3D point cloud with RGB spectral information can be projected onto the plane. Assume that a projection plane $\overrightarrow{N} \bullet P = d$ is chosen, where $\overrightarrow{N} = [a\ b\ c]$ is the normal vector. The projected coordinates P_p of a 3D point $P = [x\ y\ z]$ can be derived by Eq. (1):

$$P_p = P - \overrightarrow{N}^{*}\frac{a^*x + b^*y + c^*z + d}{norm(\overrightarrow{N})^2} \tag{1}$$

Since the LiDAR point cloud was dispersed, the projected points were rasterized regarding the ground sampling distance (GSD) of the